AIS-based Coordinated and Adaptive Control of Generator Excitation Systems for an Electric Ship

Chuan Yan, *Member, IEEE*, Ganesh K. Venayagamoorthy, *Senior Member, IEEE*, and Keith Corzine, *Senior Member, IEEE*

***Abstract*—An artificial immune system (AIS) based control of generator excitation systems for the Navy's electric ship is presented in this paper to solve power quality problems caused by high-energy loads such as direct energy weapons. The coordinated development of the AIS controllers mainly consists of two parts – innate immunity (optimal) and adaptive immunity. The parameters of the controllers for the former, to provide optimal performance, are determined simultaneously using particle swarm optimization (PSO). For dramatic changes in the ship's power system, adaptive control based on the immune system feedback law is developed. The feedback law adapts the controllers' parameters only during transient disturbances. Post-disturbance, the controllers' parameters are restored to their innate values. A ship's real-time power system and the proposed AIS control of all excitation systems have been implemented on a real-time digital simulator and digital signal processor, respectively. Results from the hardware-in-the-loop studies show that the AIS controllers can provide effective control of all generators' terminal voltages during pulsed loads, restoring and stabilizing them quickly.**

***Index Terms*—Electric ship, artificial immune system (AIS), particle swam optimization (PSO), pulsed loads.**

I. Introduction

THE Navy's Future Electric ship's power system is based on the integrated power system (IPS) architecture consisting of four parts: power generation, propulsion systems, hydrodynamics, and a DC zonal electric distribution system (DC-ZEDS), all of which provide benefits for flexibility, survivability, capability for high energy loads and maintainability [1]. In order to maintain power quality in an IPS, immediate energy storage devices, with their corresponding charging systems, are proposed to make the pulsed power required compatible with the supply system [1].

Manuscript received April 1, 2010. Accepted for publication December 14, 2011.

The financial support for this research from the US Office of Naval Research 2007 Young Investigator Award to Dr. Venayagamoorthy is gratefully acknowledged (contracting number – N00014-07-1-0806) and the US National Science Foundation CAREER grant #0348221.

C. Yan is with the Trane Residential Solution, Tyler, TX, 75707 USA (e-mail: chuan.yan@irco.com).

G. K. Venayagamoorthy is with the Holcombe Department of Electrical and Computer Engineering, Clemson University, Clemson, SC, 29634, USA (e-mail: gkumar@ieee.org).

K. Corzine is with the Missouri University of Science and Technology, Rolla, MO 65409 USA (e-mail: corzinek@mst.edu).

However, this will increase the system's cost and demand larger ship space. The excitation control is one of the most effective and economical techniques for stabilizing the terminal voltage of the synchronous generators. An optimally-tuned excitation system benefits overall operating performance during transient conditions caused by system faults, disturbance, or motor starting [2]. In order to optimize them, many algorithms are extended to the design of the optimal excitation controller for the synchronous generators. The two predominantly-used methods are the pole-placement method and the cancellation approach [2]. However, the transfer function and the parameters of the machines are needed, and they are not optimally oriented. In [3], Lyapunov's direct method has been used to optimize the excitation controller. In [4], a robust controller is proposed based on the block control technique combined with a sliding-mode control approach. In [27], a backstepping based control approach is proposed. Again, machine parameters are needed.

Recently, computational intelligence methods have been used widely in optimizing excitation controllers such as fuzzy set theory [5], particle swarm optimization (PSO) theory [6], and online trained neurocontrollers [7], all of which perform well at maintaining the terminal voltage. However, computational intelligence (CI) based controller designs use fitness functions mainly based on rise time, settling time and overshoot. Reactive power control in a multimachine power system is essential for improved system performance and minimization of power losses. Besides, an optimal excitation controller developed using CI techniques can only provide optimal performance for the range of operation conditions considered in the design. However, because its performance degrades when the operation condition changes, adaptive excitation controllers are used [8, 9]. Furthermore, the design of multiple excitation controllers to provide optimal performance with changing operating conditions is a challenging task, and one that is critical for Navy applications. This requires the coordinated development of the excitation controllers and adaptive online operation.

In this paper, an artificial immune system (AIS) based control of excitation controllers for the electric ship is presented. There are three main advantages of this control: optimal orientation, multi-machine coordinated control and adaptability. There are two parts in the AIS-based excitation control design, namely innate immunity and adaptive immunity. The parameters of the controllers for innate immunity, to provide optimal performance, are determined simultaneously using particle swarm optimization (PSO). For dramatic changes in the ship's power system, an adaptive

control based on the immune system feedback law is developed. The feedback law adapts the controllers' parameters only during transient disturbances. Post-disturbance, the controllers' parameters are restored to their innate values. A ship's power system, consisting of four generators, and the proposed AIS control of all excitation systems have been implemented on a real-time digital simulator (RTDS) and DSP, respectively. Results of the hardware-in-the-loop (HIL) studies are presented to show that four AIS controllers can provide effective control of voltages on the ship's power system during pulsed loads, restoring and stabilizing them quickly.

The remainder of the paper is organized as follows: Section II describes the ship's power system; Section III provides a detailed description of the AIS-based excitation control development; Section IV presents the HIL results, and, finally, Section V provides a conclusion.

II. Excitation Control System on an Electric Ship

A. Integrated Power System (IPS) for the Electric Ship

The power system of the all-electric ship mainly consists of two 36MW main turbine generators (MTGs), two 4MW auxiliary turbine generators (ATGs), two 36.5MW advanced induction motors (IM), ship service loads, pulsed loads and other auxiliary loads [1]. In this system, four 2MW DC zonal loads and two pulsed loads, namely a rail gun with 40MW and 0.75s duration and an EM launcher with 10MW and 3s duration, are implemented as shown in Fig. 1 [10]. The rated powers for the main and auxiliary generators are 45MVA and 5MVA, respectively. The rating and parameters in p.u. for the main and auxiliary generators are shown in Table I.

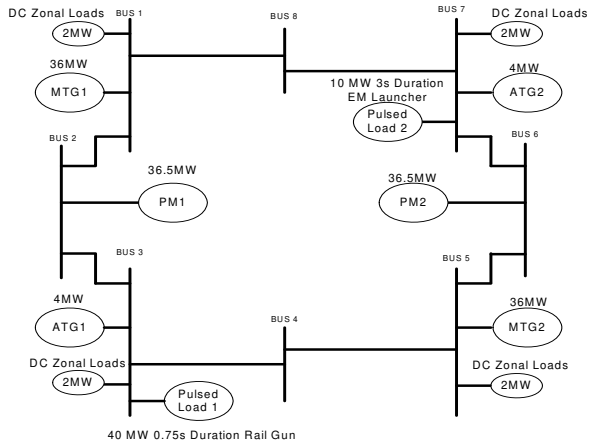

Fig. 1. IPS of an electric ship. (ATG: auxiliary turbine generator; MTG: main turbine generator; PM: Propulsion motor)

B. Excitation System

The ship's power system is small and isolated. The distance between the different power system elements is small enough that the cable inductances can be neglected. In this case, the terminal voltage of four generators is the same, which means all four generator excitation controllers respond to the same voltage feedback from the system. For reduced maintenance, all four generators are equipped with brushless exciters [11]. The excitation voltage is controlled by an automatic voltage regulator (AVR) that senses the terminal voltage of the generator and compares it with a reference value in order to regulate the terminal voltage of generators. A simplified AVR block diagram is shown in Fig. 2 [12].

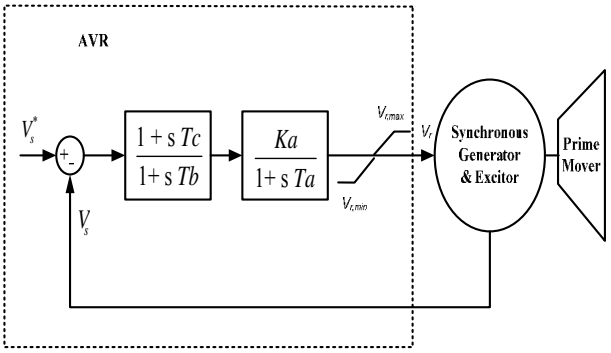

Fig.2. A simplified AVR block diagram

As shown in Fig. 2, V_s^* is the rms terminal voltage reference of the synchronous generator, and V_s is the measured value. The rms line-to-neutral terminal voltage is calculated in terms of instantaneous quantities using

$$V_s = \frac{\sqrt{v_{as}^2 + v_{bs}^2 + v_{cs}^2}}{\sqrt{3}} \quad (1)$$

The subtraction of V_s^* and V_s produces an error voltage signal, which is amplified in the regulator. The overall equivalent gain and the time constant associated with the regulator are simulated by K_a and T_a, respectively. The time constants, T_b and T_c, may be used to model equivalent time constants inherent in the voltage regulator. $V_{r,max}$ and $V_{r,min}$ define the maximum and minimum voltage regulator output, respectively. [12]

C. Hardware-in-the-Loop Laboratory Setup

In order to validate the proposed AIS excitation controls, a detailed model of an electric ship's IPS is simulated in real-time on an RTDS, which can closely replicate the dynamics of the physical ship's power system. The RTDS is equipped with D/A cards and A/D cards with a range from -10V to +10V. AIS controllers are implemented on an Innovative M67 DSP. An HIL system between the RTDS and the DSP as shown in Fig. 3 is developed. This is realized using the RTDS 16-bit D/A cards to send the four generators' terminal voltage and reactive power signals to the DSP 16-bit A/D cards at a 1 KHz sampling frequency. The digital excitation controllers of the four generators are implemented on the DSP. The DSP 16-bit D/A cards send calculated field voltages for the respective generators to RTDS 16-bit A/D cards at a 1 KHz sampling frequency.

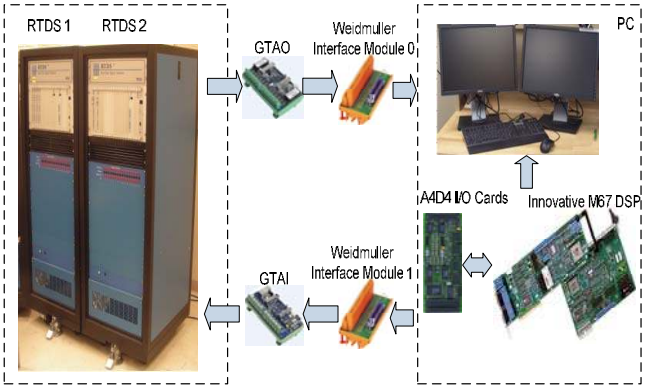

Fig. 3. HIL laboratory setup including RTDS and M67 DSP

TABLE I
MAIN SYNCHRONOUS MACHINE RATINGS AND PARAMETERS.

Power 45 MVA		Frequency 60 Hz	
voltage 13.8 kV			
X_a=0.08 pu	X_d=1.352 pu	X_d'=0.296 pu	X_d''=0.148 pu
X_q=0.836 pu	X_q''=0.122 pu	R_a=0.006 pu	T_{do}'=4.141 pu
T_{do}''=0.027 pu	T_{qo}''=0.184 pu		

III. AIS-BASED EXCITATION CONTROLLER

A. *Biological Immune System and Artificial Immune System*

The biological immune system of human beings is a complex adaptive system. The interaction of various cells within the system has evolved to protect them from invading pathogens. Antigen presenting cells (*APC*) identify the invading antigens and activate *CD4+T* cells to clone and differentiate into activated helper *T* cells (*TH cell*), which stimulate the *B cells.* Then, *B* cells will produce antibodies (A_b) to kill the antigens. When the number of antigens is reduced, suppressor *T* cells (*TS Cell*) are activated to suppress the action of *TH Cell*. The process of the biological immune system is illustrated in Fig. 4 [13-14].

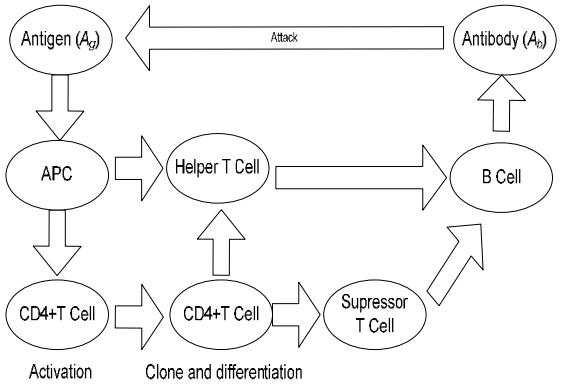

Fig. 4. Schematic showing the process of a typical biological immune system.

The AIS is a biologically motivated information processing system that has many superior optimization characteristics, such as flexible adaptability, clone selection, pattern recognition and distributed multi-level structure [15, 26]. There are two parts in an AIS-based controller design, namely innate immunity and adaptive immunity, which are described in following two subsections. Innate immunity provides optimal control with its fixed parameters, and adaptive immunity provides adaptive control with parameter variation.

B. *AIS-Based Excitation Control: Innate Immunity Design*

Innate immunity for excitation systems requires optimal controllers, which can be obtained using any optimally orientated method. In this paper, particle swarm optimization is used to find the optimal AVR parameters for the innate immunity design. Although some other computational intelligence algorithms have better average convergence, such as the clonal selection algorithm, its easy hardware implementation ability and fast global best search ability make PSO suitable for this study [24]. PSO is a swarm intelligence technique (a search method based on nature-inspired systems). It is an efficient method for solving complex nonlinear optimization problems [16-19] and has been widely used in power electronics applications to power systems [20-22]. PSO begins with a population of random particles, which are given some random positions and velocities in the search space. The particles have memory, which is used to keep track of their previous best position local best (P_{best}) and the corresponding fitness. The swarm has a memory that keeps track of the best value of all P_{best}. The search process is aimed at accelerating each particle towards its P_{best} and the swarm's global best (G_{best}). The velocity and position update equations of the particles are given by

$$v_i(j+1) = w \cdot v_i(j) + c_1 \cdot R_1 \cdot \left(P_{best}(j) - x(j)\right) + c_2 \cdot R_2 \cdot \left(G_{best} - x(j)\right) \quad (2)$$

$$x_i(j+1) = x_i(j) + v_i(j+1) \quad (3)$$

where i is the particle number, w is the inertia constant, c_1 and c_2 are the cognitive and social acceleration constants, respectively, and $R_1$and R_2 are two random numbers with uniform distribution in the interval [0,1].

Due to the symmetry of the IPS, two excitation controllers' parameters for the main generators are the same, as are those of the two auxiliary generators. Therefore, two AVRs consisting of eight parameters (K_{a_main}, T_{a_main}, T_{b_main}, T_{c_main}, K_{a_aux}, T_{a_aux}, T_{b_aux}, T_{c_aux}) serve as the PSO particle dimensions.

Initialization: Randomly initialize a population N of particles' positions and velocities. To have a fast PSO search performance, in the laboratory setup, set N as 30 and keep the values of w, c_1 and c_2 fixed at 0.8, 2.0 and 2.0 [22]. The initialization range for parameters is obtained by trial and error, which can make the system stable. K_a is from 0 to 1000; T_a ranges from 0 to 2; T_b ranges from 0 and 20; T_c ranges from 0 to 5.

Evaluation: In the excitation control loop shown in Fig. 2, the proportional gain K_a and time constants T_a, T_b and T_c must be carefully selected to provide satisfactory performance under normal and pulsed load conditions. The objective of the PSO algorithm is to find these parameters in order to restore and stabilize the terminal voltage quickly, especially after pulsed loads of different magnitudes and durations.

Most objective functions used for excitation controller design in the research literature involve settling time, rise time and overshoot [14, 23]. The area under the voltage curve during and post pulsed load can be calculated using (4). This can be used as a fitness function to guide the PSO design process to minimize the time response characteristics, such as rise time, overshoot and settling time.

$$Fitness = \frac{1}{2}\sum_{k=1}^{n}\{\sqrt{[V_s^* - V_s(k)]^2 + [V_s^* - V_s(k+1)]^2}\}\Delta t \qquad (4)$$

where

V^*_s reference terminal voltage value;
k sampling instant;
Δt sampling interval;
V_s measured terminal voltage;

However, it is possible that some generators could output negative reactive power while the others output positive reactive power if terminal voltage is the only factor considered during the tuning of excitation controllers. In this case, the current in the transmission line could be much higher, which means thicker wire and more heat. Therefore, a fitness function (5) that involves both terminal voltage and reactive power is preferred.

$$Fitness = \frac{1}{2}\sum_{k=1}^{n}\{\sqrt{[V_s^* - V_s(k)]^2 + [V_s^* - V_s(k+1)]^2}\}\Delta t + \left|Q_{MTG1}\right| + \left|Q_{MTG2}\right| + \left|Q_{ATG1}\right| + \left|Q_{ATG2}\right| \qquad (5)$$

where

Q_{MTG1} reactive power of MTG_1 in steady state;
Q_{MTG2} reactive power of MTG_2 in steady state;
Q_{ATG1} reactive power of ATG_1 in steady state;
Q_{ATG2} reactive power of ATG_2 in steady state;

Update: The position and velocity of the i^{th} particle is updated using (2) and (3).

In order to tune AVR parameters, three different kinds of pulsed loads are applied. The first is a 40MW pulsed load with a 0.75-second duration; the second is a 10MW pulsed load with a 3-second duration; the third is an overlap of the first two pulsed loads. In this case, the ship's excitation controller will achieve an innate immunity toward these three pulsed loads or other pulsed loads close to this range.

C. AIS-Based Excitation Control: Adaptive Immunity Design

Using the procedures explained in the previous section, all innate immunity parameters (K_{a_main}, T_{a_main}, T_{b_main}, T_{c_main}, K_{a_aux}, T_{a_aux}, T_{b_aux}, T_{c_aux}) are found using PSO. Based on these determined optimal values, the adaptive immune controller is designed. The input of the AIS controller is the deviation of the bus voltage $\Delta V(k)$ at time instant k, which can be regarded as the antigens. The objective of AIS is to minimize the antigens. Therefore, AIS activates helper T cells to eliminate antigens. The mathematical representation of this process can be shown using (6):

$$TH(k) = m_1 \times \Delta V(k) \qquad (6)$$

where

m_1 is the stimulating factor of the helper T cells;

In order to balance the AIS and suppress the action of TH cells, the TS cells are introduced. Their mathematical representation is shown inEquation (7).

$$TS(k) = m_2 \times \Delta V_s(k) \times \exp\left(-\frac{\Delta V_s(k)}{\Delta V_s(k-1)}\right) \qquad (7)$$

where

m_2 is the suppressor factor of the suppress T cells.

The B cells activated by TH cells and TS cells can be represented using (8).

$$B(k) = TH(k) - TS(k) \qquad (8)$$

The biological immune system can not only defend invading antigens but can also have a killing effect on self-antigens when the immune responses are inappropriately too high or too low [14]. Therefore, a limitation function is added, and the antibody can be represented as (9).The upper limit value and lower limit value are the upper range and lower range of the initialization range of parameters, respectively.

$$A_b(k) = Limitation\big(IN + B(k)\big) \qquad (9)$$

where

IN is the innate immunity parameter value.

Since the ship's power system includes four excitation controllers, four AIS controllers have been implemented. The schematic diagram of the AIS control for the ship's power system is shown in Fig. 5. In this figure, the input for the AIS controller of MGT1, MGT2, AGT1 and AGT2 are the deviation terminal voltages (pu) of Bus 1, 5, 3 and 7, respectively. The two main generators should perform identically, as should the two auxiliary generators; therefore, the innate immunity parameters and their constraints for AIS control of MTG1 and MTG2 are the same, as they are for AIS control of ATG1 and ATG2.

In this paper, PSO is used for tuning all eight TS suppression factors (m_2, m_4, m_6, m_8, m_{10}, m_{12}, m_{14}, m_{16}) and eight TH stimulating factors (m_1, m_3, m_5, m_7, m_9, m_{11}, m_{13}, m_{15}).

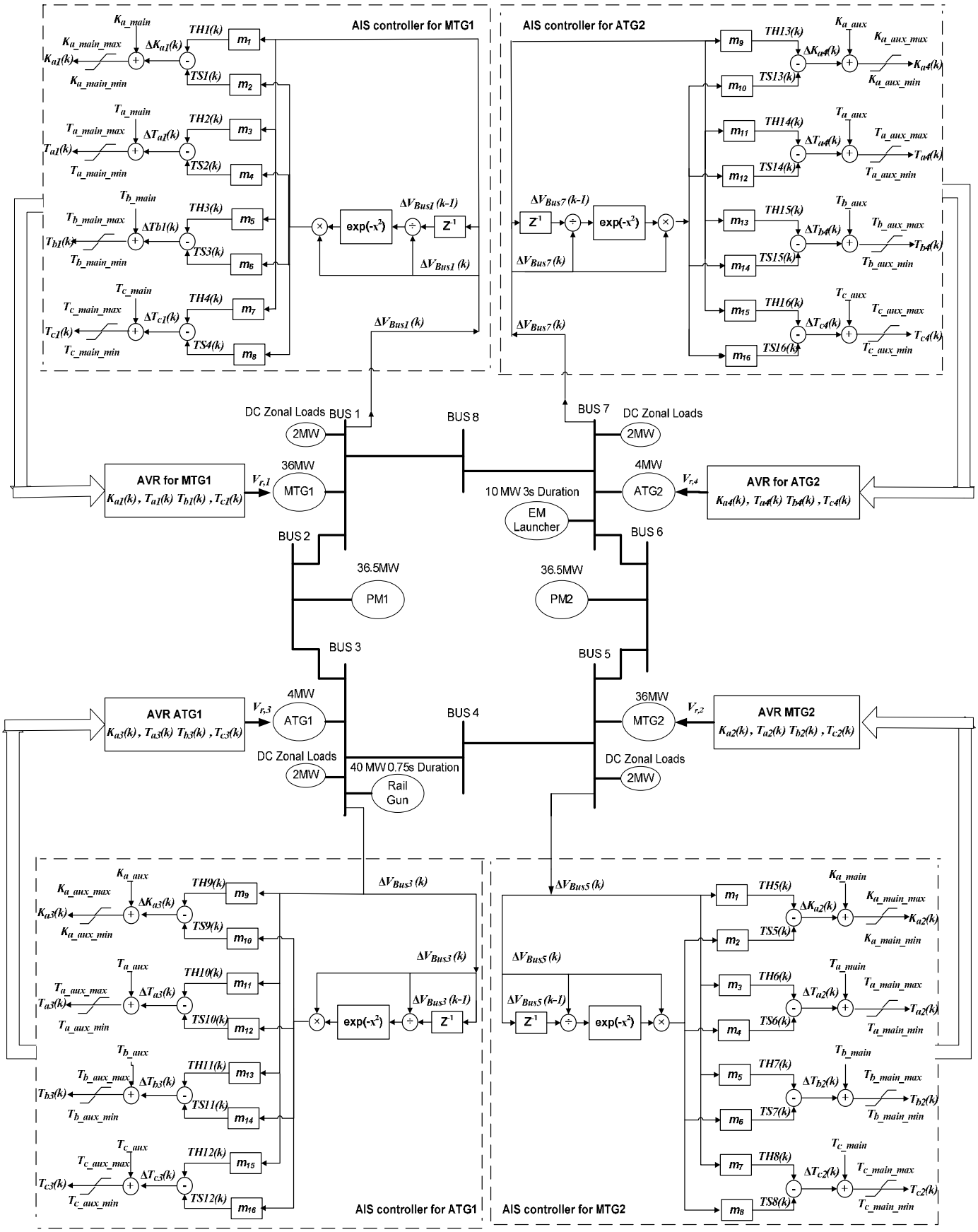

Fig. 5. Schematic of an AIS-based excitation controller for the ship's power system.

IV. Results

An AIS-based excitation controller consists of two parts: innate immunity and adaptive immunity. Innate immunity is first obtained using PSO with a presented fitness function. Then, adaptive immunity is obtained using PSO. Both innate and adaptive immunity work together to provide adaptive parameters for the excitation controller. In subsection A, the performance of the presented objective function for generator coordinate control is given. In [24], the pole placement-based controller, the predominantly used method, is compared with the PSO-based excitation controller. The results show that the PSO-based controller displays better performance than the pole-placement method-based excitation controller. In addition, although statistical analysis shows that different CI-based controllers such as PSO, CSA, population-based incremental learning (PBIL) and small population PSO (SPPSO) display different average convergence performance, their global best searching performances are similar with certain trial numbers for excitation controller tuning [24, 25]. Therefore, in subsection B, a PSO-based controller is compared with an AIS-based excitation controller because of its ease of implementation.

A. AIS-Based Excitation Controller: Innate Immunity

To verify the effectiveness of the presented fitness function for the PSO-based optimal excitation controller, two case studies have been conducted.

Case Study 1: In this study, PSO uses the fitness function given in (4) to tune the excitation controllers, while the parameters of excitation controllers for two main generators, as well as for two auxiliary generators, are set to be different. The tuned parameters of four excitation controllers for Case Study 1 are shown in Table II. The results for a 40MW and 0.75s duration pulsed load are shown in Figs. 6 through 10. The terminal voltage for four generators is shown in Fig 6. The field voltage and current are shown in Figs. 7 and 8, respectively, while the active power and reactive power for four generators are shown in Figs. 9 and 10, respectively. In Figs. 9 and 10, the field voltages and currents for four generators are different from each other, which results in different generator reactive power outputs. In this case, although the terminal voltage performs well, the power system is not balanced. Some machines are stressed while others are not, which is not desirable. Therefore, it is necessary to set the excitation controllers for two main generators, as well as for the two auxiliary generators, to be equal. In Fig. 10, although the terminal voltage performance is good and the active and reactive loads are constant, auxiliary generator 2 is absorbing reactive power because there are no reactive power constraints, which means other generators need to inject more reactive power. In this case, the current flowing through the transmission cables will be higher, and the heat and power loss will be greater. Therefore, reactive power must be taken into consideration in the fitness function as shown in (5).

TABLE II
Parameters Of The Optimal Excitation Controllers Using (4)

	Excitation controller for MTG 1	Excitation controller for MTG 2	Excitation controller for ATG 2	Excitation controller for ATG 2
K_A	430.422	676.4943	594.107	301.825
T_A	0.0675	0.001	0.230	0.574
T_B	16.603	10.515	10.000	10.000
T_C	1.010	1.000	1.000	1.000

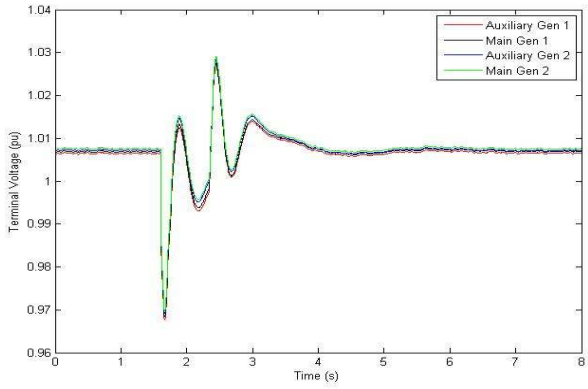

Fig. 6. Terminal voltage responses of the generators for a rail gun pulsed load with excitation controllers' parameters obtained from PSO tuning using the fitness function given in (4).

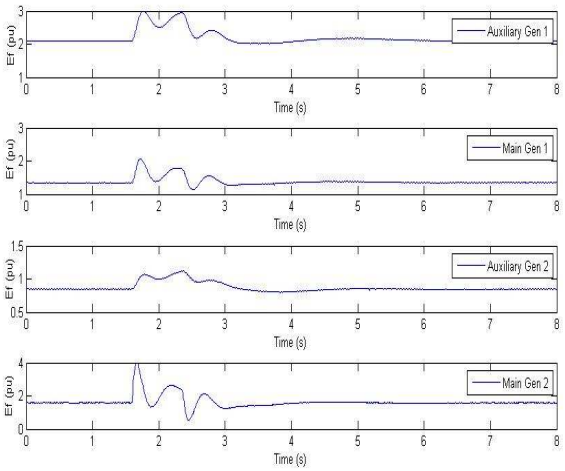

Fig. 7. Field voltages for a rail gun pulsed load with excitation controllers' parameters obtained from PSO tuning using the fitness function given in (4).

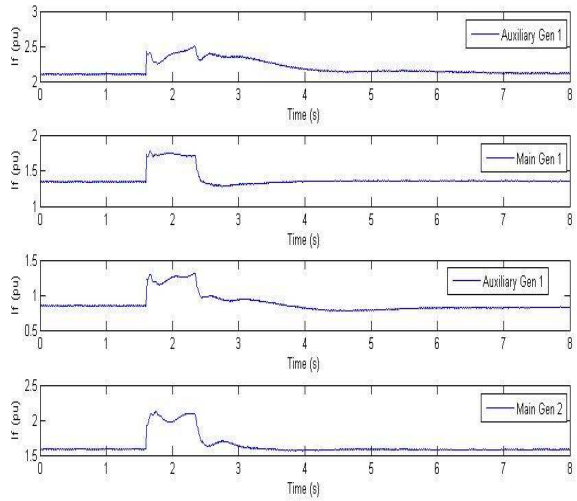

Fig. 8. Field currents for a rail gun pulsed load with excitation controllers' parameters obtained from PSO tuning using the fitness function given in (4).

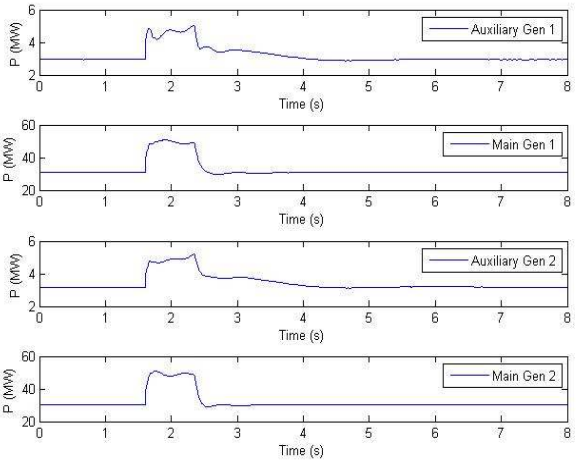

Fig. 9. Active power outputs of the generators for a rail gun pulsed load with excitation controllers' parameters obtained from PSO tuning using the fitness function given in (4).

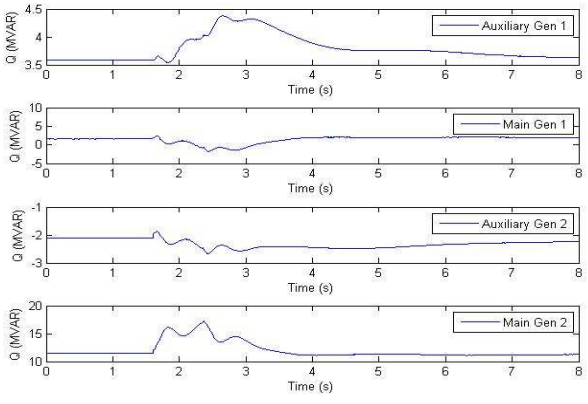

Fig. 10. Reactive power outputs of the generators for a rail gun pulsed load with excitation controllers' parameters obtained from PSO tuning using the fitness function given in (4).

Case Study 2: In this case study, fitness function (5) is used for the PSO-based tuning of excitation controllers' parameters. The parameters of the two main generators' excitation controllers, as well as those of the two auxiliary generators, are set to be identical. The tuned parameters of four excitation controllers for Case Study 2 are shown in Table III. The results for a 40MW and a 0.75s duration pulsed load are shown in Figs. 11 through 15. The terminal voltage of the four generators is shown in Fig 11. The field voltages and currents are shown in Figs. 12 and 13, respectively, while the active and reactive powers of the four generators are shown in Figs. 14 and 15, respectively.

TABLE III
PARAMETERS OF THE OPTIMAL EXCITATION CONTROLLERS USING (5)

Excitation controller for MTG 1&2		Excitation controller ATG 1&2	
K_{A_MAIN}	501.5	K_{A_AUX}	498.6
T_{A_MAIN}	0.001	T_{A_AUX}	0.246
T_{B_MAIN}	8.106	T_{B_AUX}	12.168
T_{C_MAIN}	1.299	T_{C_AUX}	1.305

Fig. 15 shows that the reactive powers of the four generators are positive and that the system is balanced, unlike in Case Study 1. Therefore, fitness function (5) is preferred.

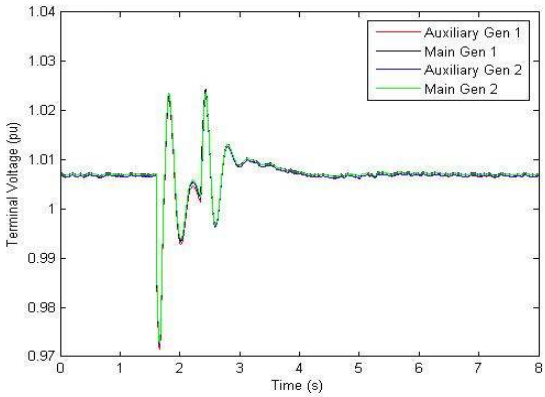

Fig. 11. Terminal voltage responses of the generators for a rail gun pulsed load with excitation controllers' parameters obtained from PSO tuning using the fitness function given in (5).

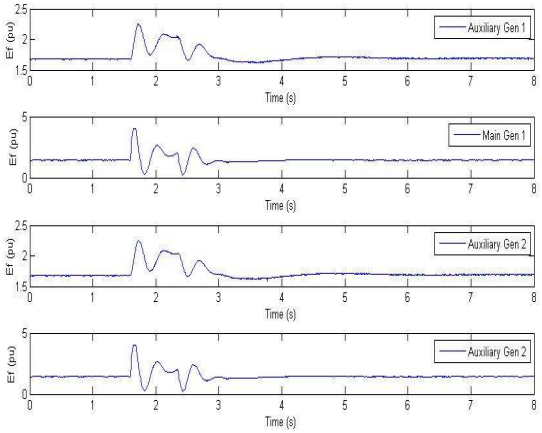

Fig. 12. Field voltages for a rail gun pulsed load with excitation controllers' parameters obtained from PSO tuning using the fitness function given in (5).

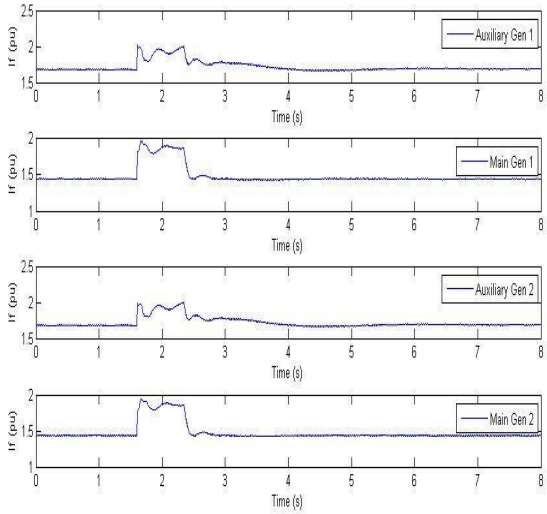

Fig. 13. Field currents for a rail gun pulsed load with excitation controllers' parameters obtained from PSO tuning using the fitness function given in (5).

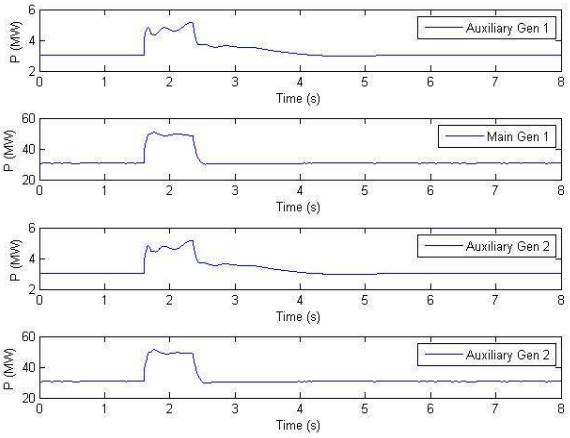

Fig. 14. Active power outputs of the generators for a rail gun pulsed load with excitation controllers' parameters obtained from PSO tuning using the fitness function given in (5).

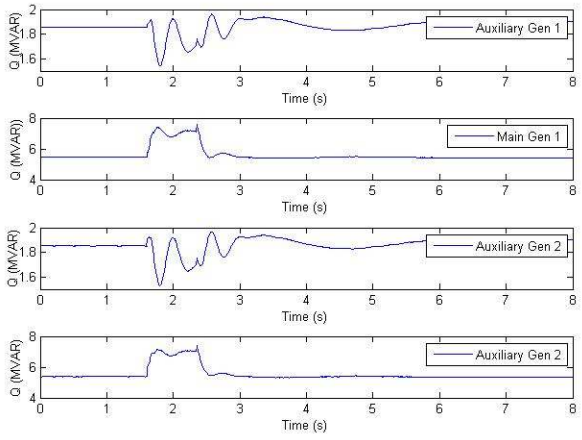

Fig. 15. Reactive power outputs of the generators for a rail gun pulsed load with excitation controllers' parameters obtained from PSO tuning using the fitness function given in (5).

B. AIS-Based Excitation Controller: Adaptive Immunity

To verify the effectiveness of the AIS-based controllers, several comparisons between AIS-based controllers and PSO-based optimal excitation controllers have been made in Table III. The stimulating and suppression factor (*m* constant) parameters obtained by PSO are shown in Table IV.

TABLE IV
PARAMETERS FOR TH STIMULATING AND TS SUPPRESSOR FACTORS

TH stimulating factors		*TS* suppressor factors	
m_1	5785.394	m_2	27918.073
m_3	3.052	m_4	8.3012
m_5	112.832	m_6	149.644
m_7	15.715	m_8	12.244
m_9	5987.508	m_{10}	28731.390
m_{11}	100	m_{12}	91.528
m_{13}	135.809	m_{14}	99.147
m_{15}	16.235	m_{16}	13.470

A detailed comparison using a 40MW pulsed load with a 0.75s duration has been made in Figs. 16 through 20. The comparison of terminal voltages for two controllers is shown in Fig. 16, which clearly demonstrates that AIS-based controllers can reduce oscillation caused by pulsed loads better than PSO-based controllers. In Figs. 17 and 18, the dynamic variation of parameters for the AVRs of two main generators and those of two auxiliary generators has been given, respectively. Parameters adaptively vary away from their optimal innate immunity values during the pulsed load, which is regarded as an invading antigen. The variation in the magnitude of parameters is well-controlled by the stimulating and suppressor factors of the AIS controller based on the invading antigen. After the disturbance, parameters again return to their optimal innate immunity values. The comparisons of field voltage and current have been shown in Figs. 19 and 20, respectively, which show the effect of variation for parameters.

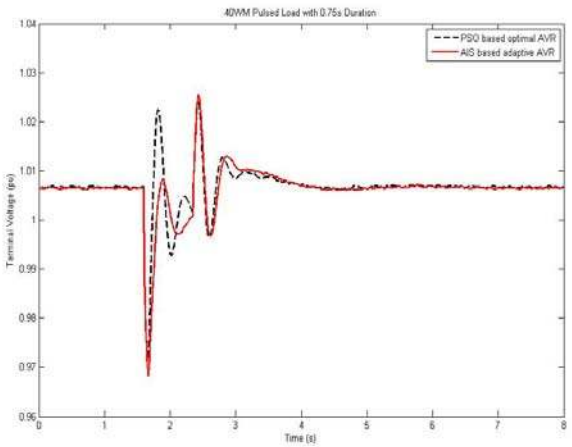

Fig. 16. Comparison of terminal voltages of a main generator for a rail gun pulsed load observed using a PSO-based optimal excitation controller and an AIS-based excitation controller.

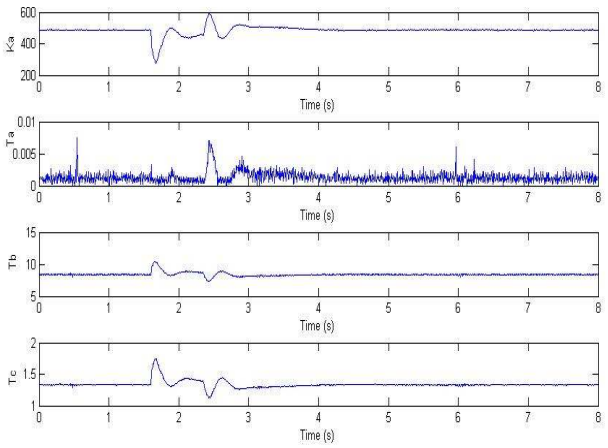

Fig. 17. Dynamic variation of parameters of an excitation controller of a main generator for a rail gun pulsed load observed using a PSO-based optimal excitation controller and an AIS-based excitation controller.

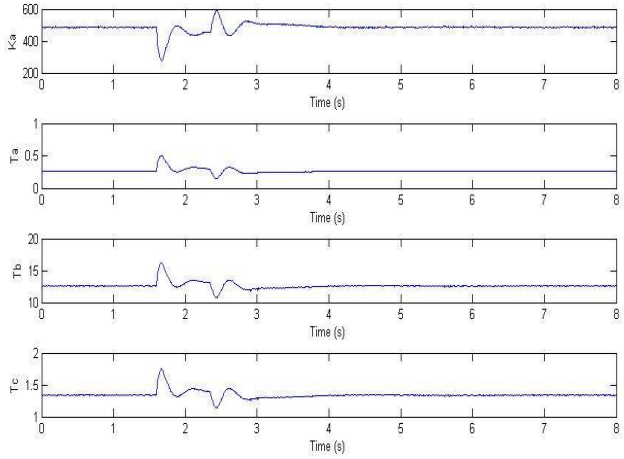

Fig. 18. Dynamic variation of parameters of an excitation controller of an auxiliary generator for a rail gun pulsed load observed using a PSO-based optimal excitation controller and an AIS-based excitation controller.

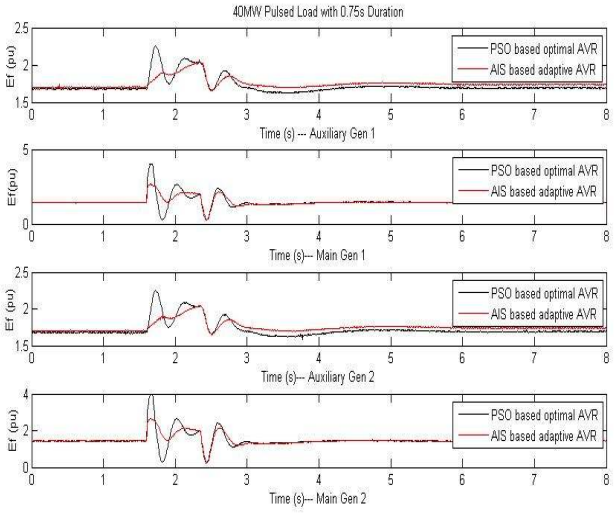

Fig. 19. Comparison of field voltages of generators for a rail gun pulsed load observed using a PSO-based optimal excitation controller and an AIS-based excitation controller.

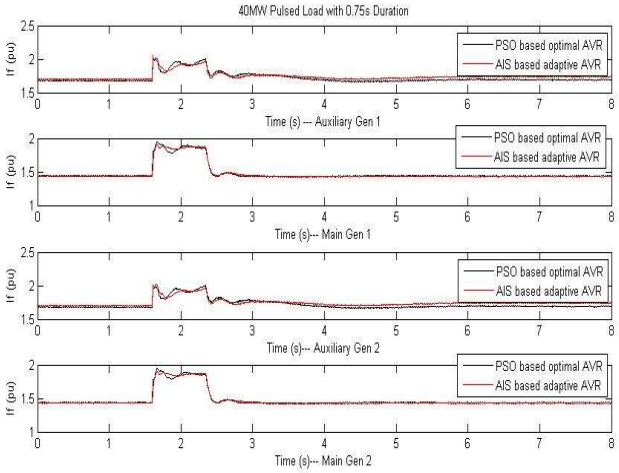

Fig. 20. Comparison of field currents of generators for a rail gun pulsed load observed using a PSO-based optimal excitation controller and an AIS-based excitation controller.

A comparison using a 10MW pulsed load with a 3s duration (EM launcher) has been made in Fig. 21, which shows that the AIS controller performs better than the PSO-based optimal controller.

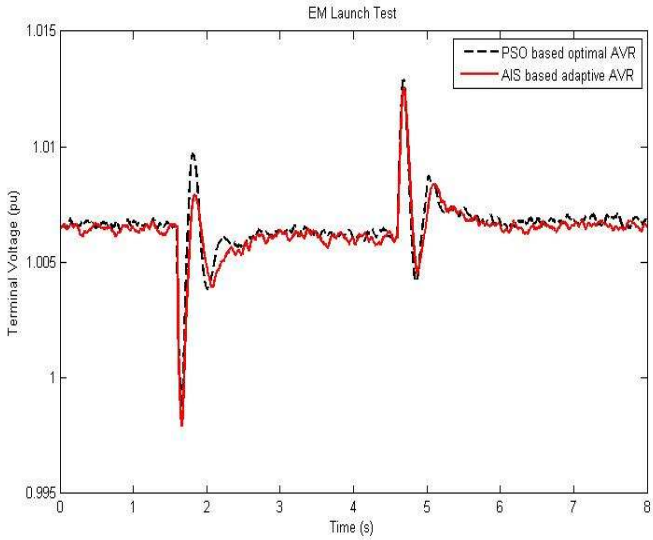

Fig. 21. Comparison of terminal voltage (system voltage) for an EM launcher pulsed load observed using a PSO-based optimal excitation controller and an AIS-based excitation controller.

Two more comparisons with different pulsed loads are shown in Figs. 22 and 23. In Fig. 22, system voltage is shown for an overlap of an EM launcher pulsed load and a 40WM, 0.75s duration pulsed load. The EM launcher pulsed load is fired first, and after 2.25s, the other is fired. They are switched off at the same time. In Fig. 23, a comparison using a 0.75s duration pulsed load with different magnitude has been made. Figs. 16 through 23 show that the AIS-based excitation controller can perform better than the PSO-based optimal excitation controller.

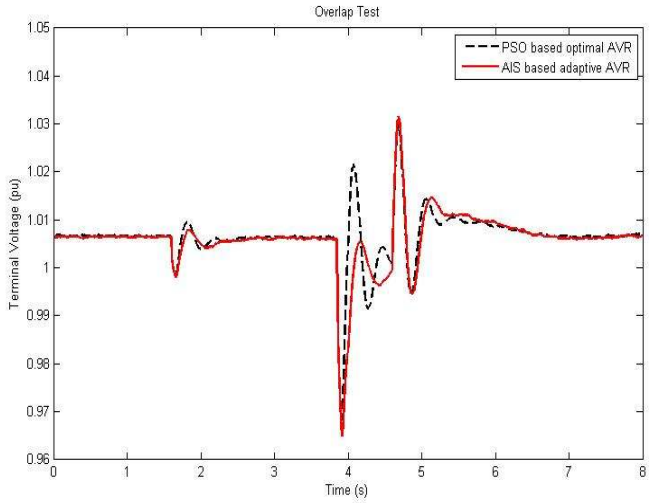

Fig. 22. Comparison of terminal voltage (system voltage) for overlapping of two pulsed loads observed using a PSO-based optimal excitation controller and an AIS-based excitation controller.

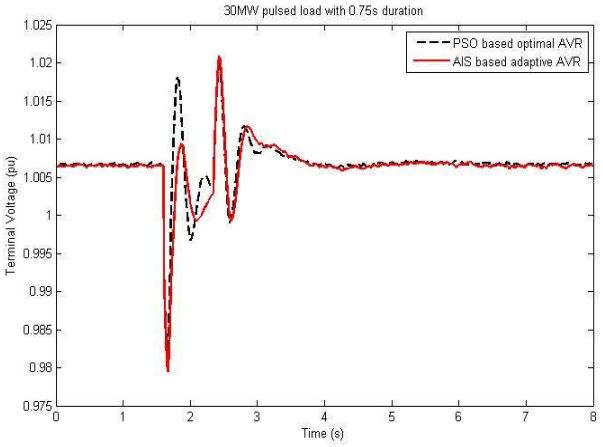

Fig. 23. Comparison of terminal voltage responses (system voltage) for a rail gun pulsed load with a 30MW and a 0.75s duration observed using a PSO-based optimal excitation controller and an AIS-based excitation controller.

V. Conclusion

Artificial immune system-based excitation controllers have been developed for an electric ship's power system. The objective of the excitation controllers is to minimize the voltage deviations and power losses when pulsed loads are directly energized by the shipboard's power system. Real-time simulation of the ship's power system on a real-time digital simulator and of the AIS controllers on an M67 Innovative DSP has been carried out. The main implementation difficulty is to find the initialization range for the controller parameters. A bad range may lead to controller instability during tuning or pre-matured solution. Because it is assumed that no machine parameters are known, the initialization range is obtained by trial and error. However, if machine parameters are given, classical methods such as root locus analysis can be employed to calculate the stable and reasonable initiation range for an AIS-based controller.

The advantages of the AIS controller structure presented in this paper are that it provides optimal performance (innate immunity) for known disturbances and it adapts its parameters for unknown disturbances to provide improved performance (adaptive immunity). Compared with the PSO-based optimal controller, the hardware-in-the-loop simulation results show that the AIS-based controller can restore and stabilize the terminal voltage effectively and very quickly after high power pulse loads are experienced. The controller design based on the fitness function, taking into account the terminal voltage (system voltage) deviation and steady state reactive power outputs of the generators, ensures that no generator is absorbing reactive power.

References

[1] L. N. Domaschk, Abdelhamid Ouroua, Robert E. Hebner, "Coordination of Large Pulsed Loads on Future Electric Ships," *IEEE Transaction on Magnetics*, vol. 43, no.1, January 2007.

[2] K. Kim, R. C. Schaefer, "Tuning a PID Controller for a Digital Excitation Control System," *IEEE Transactions on Industry Application*, vol.41, no.2, pp.485-492, March/April 2005.

[3] J. Machowski, S. Robak, J. W. Bialek, J. R. Bumby, N. AbiSamra, "Decentralized Stability-Enhancing Control of Synchronous Generator," *IEEE Transactions on Power Systems*, vol.15, no.4, November 2000.

[4] A.G. Loukianov, J.M. Cañedo, L.M. Fridman, A. Soto-Cota, "High-Order Block Sliding-Mode Controller for a Synchronous Generator With an Exciter System," *IEEE Transaction on Industrial Electronics*, vol. 58, no. 1, pp. 337–347, 2011.

[5] F. Zheng, Q. Wang, T. H. Lee, and X. Huang, "Robust PI Controller Design for Nonlinear Systems via Fuzzy Modeling Approach," *IEEE Transactions on Systems, Man, and Cybernetics*, vol.31, no.6, November 2001.

[6] Ali Karimi, Ali Feliachi, "PSO-tuned Adaptive Backstepping Control of Power Systems," *IEEE Power Systems Conference and Exposition*, pp. 1315-1320, October 2006.

[7] S.Mohagheghi, Y. del Valle, G. K. Venayagamoorthy, and R. G. Harley, "A proportional-integrator type adaptive critic design-based neurocontroller for a static compensator in multimachine power systems," *IEEE Transaction on Industrial Electronics*, vol. 54, no. 1, pp. 86–96, Feb. 2007.

[8] K. Wang, H. Xin and D. Gan, "Robust adaptive excitation control based on a new backstepping approach," *IEEE Power & Energy Society General Meeting*, pp.1-5, 2009.

[9] O.P. Malik and G.S. Hope, "An Adaptive Generator Excitation Controller Based on Linear Optimal Control," *IEEE Transactions on Energy Conversion,* vol 5, no. 4, December 1990.

[10] D. H. Clayton, S. D. Sudhoff, and G. F. Grater, "Electric Ship Drive and Power System," Conference Record of the 2000 Twenty-fourth International Modulator Symposium, pp.85-88, 2000.

[11] J. F. Gieras, (2009). *Advancements in Electric Machines*, Springer.

[12] IEEE Standard 421.5, *2005 IEEE Recommended Practice for Excitation System Models for Power System Stability Studies*, pp. 1-85, 2006.

[13] H.F. Wang, H. Li and H. Chen, "Power System Voltage Control by Multiple STATCOMs Based on Learning Humorial Immune Response", *IEE Proceedings of Generation, Transmission and Distribution*, vol. 149, no. 4, pp. 416-426, 2002.

[14] P. Mitra and G.K. Venayagamoorthy, "An Adaptive Control Strategy for DSTATCOM Applications in an Electric Ship Power System," *IEEE Transactions on Power Electronics*, vol.25, no.1, pp.95-104, 2010.

[15] Y.X. Liao, J.H. She and M. Wu, "Integrated Hybrid-PSO and Fuzzy-NN Decoupling Control for Temperature of Reheating Furnace," *IEEE Transactions on Industrial Electronics,* vol.56, no. 7, pp.2704-2714, July 2009.

[16] S.H. Ling, H. Lu, F.H.F. Leung and K.Y. Chan, "Improved Hybrid Particle Swarm Optimized Wavelet Neural Network for Modeling the Development of Fluid Dispensing for Electronic Packaging," *IEEE Transactions on Industrial Electronics,* vol.55, no. 9, pp.1478-1489, September 2008.

[17] A. Chatterjee, K. Pulasinghe, K. Watanabe and K. Izumi, "A particle-swarm-optimized fuzzy-neural network for voice-controlled

robot systems," *IEEE Transactions on Industrial Electronics,* vol.52, no. 6, pp.1478-1489, December 2005.

[18] C. Dai, W. Chen and Y. Zhu, "Seeker Optimization Algorithm for Digital IIR Filter Design," *IEEE Transactions on Industrial Electronics,* accepted for future publication, vol. 57, no. 5, pp. 1710-1718, 2009.

[19] C.-H. Liu, Y.Y. Hsu, "Design of a Self-Tuning PI Controller for a STATCOM Using Particle Swarm Optimization," *IEEE Transactions on Industrial Electronics,* accepted for future publication, vol. 57, no. 2, pp. 702-715, 2009

[20] N. He, D. Xu and L. Huang, "The Application of Particle Swarm Optimization to Passive and Hybrid Active Power Filter Design," *IEEE Transactions on Industrial Electronics,* vol.56, no. 8, pp.2841-2851, August 2009.

[21] F.-J. Lin, L.-T. Teng, J.-W. Lin and S.-Y. Chen, "Recurrent Functional-Link-Based Fuzzy-Neural-Network-Controlled Induction - Generator System Using Improved Particle Swarm Optimization," *IEEE Transactions on Industrial Electronics,* vol. 56, no. 5, pp.1557-1577, May 2009.

[22] Y. del Valle, G.K. Venayagamoorthy, S. Mohagheghi, J.C. Hernandez and R.G. Harley, "Particle Swarm Optimization: Basic Concepts, Variants and Applications in Power Systems," *IEEE Transactions on Evolutionary Computation*, vol. 12, no. 2, pp.171-195, April 2008.

[23] E.R.C. Viveros, G. N. Taranto and D.M. Falcao, "Tuning of Generator Excitation Systems using meta-heuristics," *IEEE Power Engineering Society General Meeting*, pp. 1-6, 2006.

[24] C. Yan, G. K. Venayagamoorthy and K.A. Corzine, "Hardware Implementation of an AIS-Based Optimal Excitation Controller for an Electric Ship," *IEEE Transactions on Industrial Application,* vol. 47, no. 2, pp. 1070-1070, 2011.

[25] P. Mitra, C. Yan, L. Grant, G. K. Venayagamoorthy and K. Folly, "Comparative Study of Population Based Techniques for Power System Stabilizer Design," *International Conference on Intelligent System Applications to Power Systems*, pp.1-6, 2009.

[26] M.R. Widyanto, B. Kusumoputro, H. Nobuhara, K. Kawamoto and K. Hirota, "A Fuzzy-similarity-based self-organized network inspired by immune algorithm for three-mixture-fragrance recognition," *IEEE Transactions on Industrial Electronics,* vol.53, no.1, pp. 313-321, 2005.

[27] Y. Wang and X. Yu, "New Coordinated Control Design for Thermal-Power-Generation Units," *IEEE Transactions on Industrial Electronics,* vol.57, no.11, pp. 3848-3856, 2010.

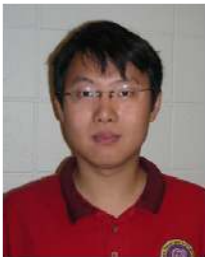

Chuan Yan (S'08-M'10) received his B.S. degree in electrical engineering from Lanzhou University of Technology, China in 2005 and the M.S. degree in electrical engineering from Chongqing University, China in 2008. He received his Ph.D degree in the electrical engineering from Missouri University of Science and Technology (Missouri S&T), US in 2010.

He was a postdoctoral fellow at Real-Time Power and Intelligence System lab (RTPIS) at Missouri S&T in 2010. He is currently a senior power electronics engineer at Trane Residential Solution. His research interests include motor drives, electric machinery analysis, and computational algorithms for power systems stability and control.

Ganesh Kumar Venayagamoorthy (S'91, M'97, SM'02) received his Ph.D. degree in electrical engineering from the University of Natal, Durban, South Africa, in 2002. He is the Duke Energy Distinguished Professor of Electrical and Computer Engineering at Clemson University, Clemson, USA. Prior to that, he was a Professor of Electrical and Computer Engineering at the Missouri University of Science and Technology (Missouri S&T), Rolla, USA. He was a Visiting Researcher with ABB Corporate Research, Sweden, in 2007. Dr. Venayagamoorthy is Founder and Director of the Real-Time Power and Intelligent Systems Laboratory (http://rtpis.org). His research interests are in the development and applications of advanced computational algorithms for real-world applications, including power systems stability and control, smart grid applications, sensor networks and signal processing. He has published 2 edited books, 6 book chapters, and over 90 refereed journals papers and 290 refereed conference proceeding papers.

Dr. Venayagamoorthy is a recipient of several awards including a 2008 US National Science Foundation (NSF) Emerging Frontiers in Research and Innovation Award, a 2007 US Office of Naval Research Young Investigator Program Award, a 2004 NSF CAREER Award, the 2010 Innovation Award from St. Louis Academy of Science, the 2010 IEEE Region 5 Outstanding Member Award, the 2006 IEEE Power and Energy Society Outstanding Young Engineer Award, the 2005 South African Institute of Electrical Engineers (SAIEE) Young Achievers Award, and the 2003 International Neural Network Society's Young Investigator Award.

Dr. Venayagamoorthy has been involved in the leadership and organization of many conferences including the Chair of the 2011 IEEE Symposium of Computational Intelligence Applications in Smart Grid (CIASG). He is currently the Chair of the IEEE PES Working Group on Intelligent Control Systems, the Founder and Chair of IEEE Computational Intelligence Society (CIS) Task Force on Smart Grid, and the Chair of the IEEE PES Intelligent Systems Subcommittee. He is currently an Associate Editor of the IEEE Transactions of Evolutionary Computation and an Editor of the IEEE Transactions on Smart Grid and Elsevier journal of Neural Networks. Dr. Venayagamoorthy is a Fellow of the Institution of Engineering and Technology (IET), UK, and the SAIEE.

Keith Corzine (S'92-M'97-SM'06) received his B.S.E.E., M.S.E.E., and Ph.D. degree from the University of Missouri, Rolla, in 1992, 1994, and 1997, respectively.

He was with the University of Wisconsin, Milwaukee, from 1997 to 2004, and is currently a Professor with the Missouri University of Science and Technology, Rolla. His research interests includes power electronics, motor drives, naval ship propulsion systems, and electric machinery. He has published nearly 40 refereed journal papers, over 60 refereed conference papers, and is the holder of three U.S. patents related to power conversion.